THE JOURNAL OF PHYSICAL CHEMISTRY A

ARTICLE

pubs.acs.org/JPCA

Three-Stage Transformation Pathway from Nanodiamonds to Fullerenes

Anastassia Sorkin,[†,‡] Bengkang Tay,[‡] and Haibin Su*[,†,§]

Divisions of [†]Materials Science and [‡]Microelectrics, Nanyang Technological University, 50 Nanyang Avenue, Singapore 639798, Singapore

[§]Institute of High Performance Computing, 1 Fusionopolis Way, Connexis 138632, Singapore

ABSTRACT: The dynamics of structure evolution of nanodiamonds ranging from 22 to 318 atoms of various shapes is studied by density functional tight-binding molecular dynamics. The spherical and cubic nanodiamonds can be transformed into fullerene-like structures upon heating. A number of the transformed fullerenes consist of pentagons and hexagons only. Others contain squares, heptagons, and octagons. One simulated fullerene is an isomer of C_{60}. The temperature of the transformation depends on the size, shape, and orientation of initial cluster. To be transformed into onion-like fullerenes, the spherical nanodiamonds should have 200 atoms or more, while the cubic ones require 302 atoms or more. The time-resolved energy profiles of all the transformations clearly reveal *three-stage transformation* character. During the first stage, the energy reduces quickly due to converting sp^3 carbon with dangling bond at the surface into sp^2 one, and the formation of partial sp^2 envelope wrapping the cluster. For the second stage, energy decreases slowly. The remaining interior carbon atoms come to the surface through the hole in the sp^2 envelope, and similar amount of sp^3 and sp^2 atoms coexist. The third stage involves the closure of holes, accompanied by the detachment of C_2 molecules and carbon chains from the edges. The energy decreases relatively fast in this stage. The proposed *three-stage transformation* pathway holds for all the simulations performed in this work, including those with the instant heating.

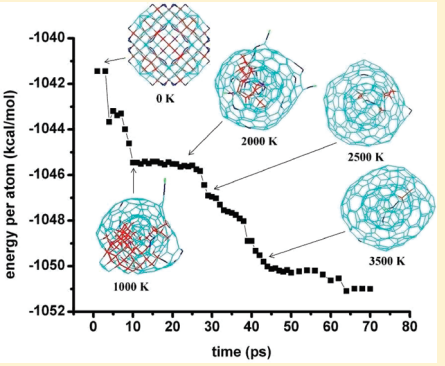

1. INTRODUCTION

Since the discovery of fullerenes in 1985,[1,2] allotropes of carbon, including CNT[3] and graphene,[4] together with their hybrid structures such as peapod,[5] nanobuds,[6] and so on, have attracted worldwide intensive attention.[7−30] The most common and the most stable are spherical fullerenes C_{60} and C_{70},[1,2,9] while the other small fullerenes have also been observed, such as C_{20},[16,21] C_{32},[17] and C_{36}.[18] Besides, the spherical carbon particles consisting of concentric graphitic shells, called carbon onions, are found in carbon soots.[10,14,15,24] Fullerenes can be formed in many processes, such as laser vaporization,[1,25] carbon arc,[2] hydrocarbon combustion,[7,8] lightning strikes,[11] asteroid impacts on Earth,[12,22] and ancient brush fires.[13] All these observations suggest that the critical condition for the formation of fullerenes from carbon-rich materials is the very high temperature. Various numerical simulations have been performed to investigate the detailed process of fullerene formation.[31−50] For example, László[35] observed formation of cage-like C_{60} cluster in helium gas atmosphere by tight-binding molecular dynamics at T_{gas} = 4000 K. Yamaguchi and Maruyama[36] studied the fullerene formation from carbon atoms in gas phase. They showed that the fullerene-like cluster could grow as big as C_{70} at the temperature ranging from 2500 to 3000 K, while the graphitic sheets were observed at lower temperature. Irle et al.[42] carried out QM/MM simulations of randomly oriented C_2 molecules under high temperature and constant flux and observed self-assembled formation of fullerene cages. Their simulations suggested that the shrinking hot giant model was the leading mechanism of the dynamic fullerene self-assembling. Lau et al.[46] simulated the formation of onion-like fullerenes within foam-like carbon at 4000 K using environment dependent interaction potential, which was used later on to study the formation of fullerenes from amorphous precursors.[49]

The stability of nanodiamond particles have been intensively studied during last two decades both experimentally[51−56] and theoretically.[37,39,57−63] Nanodiamonds with diameter around 5 nm can be transformed into spherical and polyhedron carbon onions at high temperature.[51−53] Barnard et al.[60,61] showed by means of first-principle calculations that fullerene is more stable form of nanocarbon than nanodiamond in the range 1.9−5.2 nm of diameter. Raty et al.[62,63] also used ab initio calculations to show that nanodiamonds consist of a diamond core and a reconstructed fullerene-like surface. From the perspective of the transformation pathway, Fugaciu et al.[37] studied diamond nanoparticles of 1.2 to 1.4 nm diameter by means of molecular dynamics simulations with density functional tight-binding method. They observed formation of concentric shell fullerenes

Received: January 16, 2011
Revised: June 9, 2011
Published: June 25, 2011

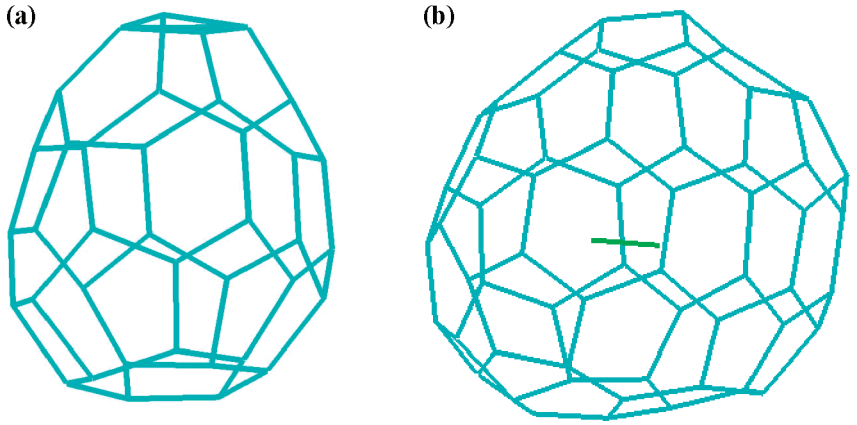

Figure 1. One fullerene with 38 atoms (a) and an isomer of the classical fullerene C_{60} (I_h) with C_2 inside.

at temperature from 1400 to 2800 K. However, their biggest diamond nanoparticles consisting of 191 and more atoms did not transform completely within the limited simulation time. The intershell spacing was below the interlayer distance of graphite. Some of the onion-like fullerenes had sp^3-like cross-links between the shells. Lee et al.[39] performed tight-binding molecular dynamics simulation of a nanodiamond of diameter ~1.4 nm under high temperature above 2500 K, and found that the nanodiamond cluster transforms into a tube-shaped fullerene via annealing. These authors showed that the "flow-out" mechanism of the transformation prevails at the temperature below 2500 K and the "direct adsorbtion" and "push-out" mechanism are observed at higher temperature. Bródka et al.[47] observed transformation of nanodiamond particles of 23 nm in diameter with the shape of truncated octahedron and sphere into onion-like carbons at 1200 and 1500 K, respectively, with REBO potential. Recently, Leyssale and Vignoles[48] investigated the time evolution of structure and internal temperature of small nanodiamond at 1500 K during the transformation to graphitized carbon onion.

Despite extensive work in this subject, as mentioned above, the boundary of forming single-shell and double-shell fullerenes is still missing, needless to mention the complete mechanism and dynamics in the whole course of transformation. Thus, it is highly desirable to carry out systematic studies on the transformation of nanodiamonds to fullerenes with different sizes and shapes. Here we present the density functional tight-binding simulation of nanodiamods with 5−14 Å in diameter and various shapes and orientations at the temperature of 2500−3500 K. The conversions of the nanodiamond particles containing more than 60 atoms into fullerene-like structures are observed. The large nanodiamonds with more than 200 atoms are transformed into onion-like carbon structures. The time-resolved structure and energy information are scrutinized to explore the mechanism and dynamics of the transformation.

2. COMPUTATIONAL METHOD

Modeling of the transformation process of diamond cluster containing more than 100 carbon atoms requires several tenths picoseconds of molecular dynamics simulations. Therefore, we apply the density-functional-based nonorthogonal Frauenheim's tight-binding model[64,65] (DFTB) implemented in the PLATO package.[66−68] In this method density-functional based scheme is used for the construction of the nonorthogonal matrix elements within the framework of linear combination of atomic orbitals formalism with the local density approximation. The method is reliable and transferable for describing carbon systems over a wide range of bonding environments.[64,69−71] The method is capable of describing the surface reconstruction of diamonds,[72,73] the electronic properties of fullerenes,[74] and carbon nanotubes.[75−77] Our calculations are carried out in NVT ensemble. Periodic boundary conditions are applied in all three directions. The Γ-point Brillouin zone sampling is used for the electronic calculations, and the MD step is 1 fs.

The spherical and cubic nanodiamonds with 5−14 Å in diameter containing different number of atoms are chosen inside a diamond network with the density of 3.5 g/cm^3. The major surfaces are chosen from {001}, {111}, and {311} surfaces of the diamond lattice. The nanodiamond cluster is put inside a supercell with 10 Å vacuum layers in x, y, and z directions, which is to eliminate the interaction between the cluster and its images generated by translational symmetry operation. First, each nanodiamond cluster is optimized at zero temperature by steepest descent method with the Frauenheim's tight-binding carbon potential. The optimization at 0 K changes the shape of small nanodiamonds. However, the shape of nanodiamonds containing 100 and more atoms commonly remains unchanged, that is, to be cubic for cubic nanodiamonds and spherical for spherical ones. Then the cluster is heated up with the heating rate of 100 K/ps using DFTB molecular dynamics. The heating is stopped when either the fullerene-like structure is formed or the temperature reaches 3500 K. The simulated structures are slowly cooled down to the room temperature at the cooling rate of 20 K/ps. Finally, the stability of these structures is confirmed by no imaginary frequency associated with the normal modes computed with the B3LYP/6-31G*[78−80] method. The visualization tools used in this work are VMD[81] and AViz[82] packages.

3. RESULTS AND DISCUSSIONS

3.1. Formation of Single-Shell Fullerenes. Most of the small nanodiamonds containing less than 60 atoms (<7 Å in diameter) lose their diamond structure at the stage of optimization. The further heating (up to 300−2000 K) converts the small nanodiamonds ranging from 20 to 30 atoms into linear chains. Most nanodiamonds containing 30−50 atoms are transformed into open-shaped sp^2-hybridized carbon objects. Only 2 out of 11 small nanodiamonds are converted into stable closed-shape

Table 1. Number of Atoms, N_1 for Initial Structure (N_2 for Final Structure), Diameters, D_1 for Initial Structure, Equatorial Diameters, D_2, and Shape and Orientation of Initial Nanodiamond Clusters with Spherical (sph) or Cubic Shape[a]

(a)

								rings				
N_1	shape	orient.	D_1 (Å)	T_1 (K)	T_2 (K)	N_2	D_2 (Å)	4	5	6	7	8
35	sph	111	5.79	0	0	31	4.40*5.29*6.14	3	5	8	1	1
42	sph	311	7.53	0	1700	38	5.35*5.75*5.74	2	9	9	1	0
63	cubic	111	7.10	0	1700	44	6.88*5.94*5.04	0	12	12	0	0
66	sph	001	7.10	2500	2800	60	7.84*6.72*6.78	0	12	20	0	0
71	sph	111	8.15	800	2200	65	7.00*8.69*7.15	0	14	17	2	1
82	sph	001	8.31	0	1900	74	8.36*7.73*7.59	0	15	21	3	0
87	sph	111	8.33	300	2300	68	8.06*6.53*7.92	0	13	22	1	0
101	cubic	001	7.98	500	1800	76	8.09*6.40*9.63	1	15	19	5	0
106	sph	001	8.88	700	2600	88	9.60*7.65*8.38	0	16	26	4	0
156	cubic	001	8.79	700	3300	121	14.32*9.44*9.14	0	20	34	6	2
172	sph	311	11.77	1000	2700	124	11.09*10.73*9.23	1	18	37	8	0
192	cubic	001	9.76	1400	2800	126	9.17*8.53*13.94	0	22	30	10	0
194	sph	111	11.77	1300	3100	158	11.13*14.01*11.18	1	15	56	7	1
220	sph	111	12.37	1500	3200	193	11.61*11.53*16.49	0	25	56	13	3
229	cubic	111	10.87	1200	2500	178	15.14*10.78*12.98	0	25	43	13	5
293	cubic	001	11.53	1800	2500	190	13.89*12.46*13.17	1	21	61	13	1

(b)

								rings				
N_1	shape	orient.	D_1 (Å)	T_1 (K)	T_2 (K)	N_2	D_2 (Å)	4	5	6	7	8
206	sph	111	12.55	1100	2400	32	4.77*5.87*4.71	1	10	7	0	0
						132	9.88*11.26*10.75	0	15	50	3	0
234	sph	111	12.84	700	2300	41	5.78*6.46*5.21	0	10	7	1	1
						171	11.74*13.69*13.29	0	20	55	7	2
239	sph	311	12.42	1400	2600	44	6.31*5.95*6.18	1	11	11	1	0
						154	11.54*11.57*12.46	2	23	35	17	1
256	sph	001	12.43	1000	2500	62	7.28*7.20*6.77	0	13	19	1	0
						186	12.93*12.91*12.19	0	25	22	12	1
302	cubic	311	11.77	600	3100	63	7.33*6.59*9.04	1	12	16	3	0
						207	13.54*12.13*14.86	0	26	64	11	2
318	sph	311	14.38	2000	3300	67	7.58*9.12*6.07	1	12	18	4	0
						221	15.34*15.27*11.23	0	34	59	15	3

[a] At temperature T_1, the inner core of nanodiamond starts to transform, and at T_2, the fullerene is formed. The single-shell fullerenes are listed in (a) and double-shell (onion-like) fullerenes in (b). For each onion-like fullerene, the first row refers to inner shell, while the second row for outer shell in D_2.

fullerenes. One of them has 31 atoms with 3 four-, 5 five-, 8 six-, 1 seven-, and 1 eight-membered rings, converted by heating the spherical (111) nanodiamond cluster with 35 carbon atoms. The presence of squares and octagons is related to the two "tails" of the fullerene. The other small fullerene consists of 38 atoms with 2 four-, 9 five-, 9 six-, and 1 seven-membered rings (see Figure 1a), obtained by hearting the spherical (311) diamond cluster with 42 atoms. When temperature reaches 1700 K, four atoms detach from the cluster. The diameter of the final product is 5.75 Å. Here we highlight one special product, which is an isomer of C_{60} (Figure 1b). The starting structure is a spherical (001) nanodiamond with 66 atoms, which is transformed into an extremely stable buckydiamond, that is, a diamond core with a reconstructed fullerene-like surface, during structural optimization. The further structural transformation does not start until 2500 K. During the transformation, two C_2 molecules detach the cluster, and another C_2 molecule remains inside the fullerene. This C_2 molecule does not attach to the interior surface of the isomer in the process of B3LYP/6-31G* optimization, which is due to the inert chemical nature of carbon atoms on the surface with positive Gaussian curvature. The final structure has a shape close to spherical and contains 20 hexagons and 12 pentagons as the classical buckminsterfullerene C_{60} (I_h). This fullerene is stable with and without C_2 inside.

All the nanodiamonds studied in this work, of any shape and orientation with 60 up to 200 atoms, are transformed into

dx.doi.org/10.1021/jp200449f |J. Phys. Chem. A 2011, 115, 8327–8334

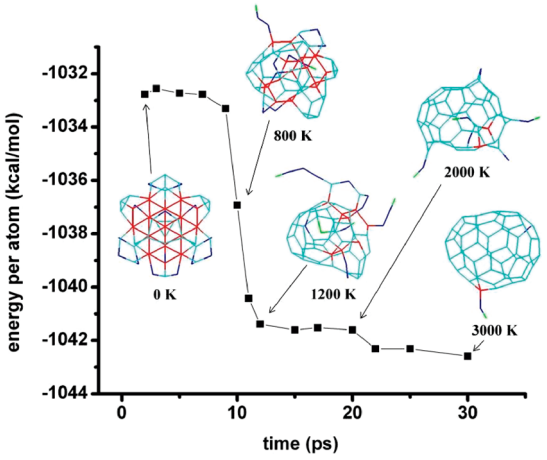

Figure 2. Structure transformation and energy profile of the spherical (111) nanodiamond cluster with 71 atoms as the initial structure. The sharp drop of energy related to the first stage of transformation occurs between 600 and 1000 K. The second stage refers to the plateau between 10 and 20 ps. The interior atoms can come outside through the hole in the sp^2 envelope. The third stage is represented by the relative fast reduction in energy from 20 ps. This stage is less clearly distinguished here due to the limited number of atoms in this small cluster. Red lines are sp^3 bonds, light blue lines are sp^2 bonds, and dark blue lines are sp bonds.

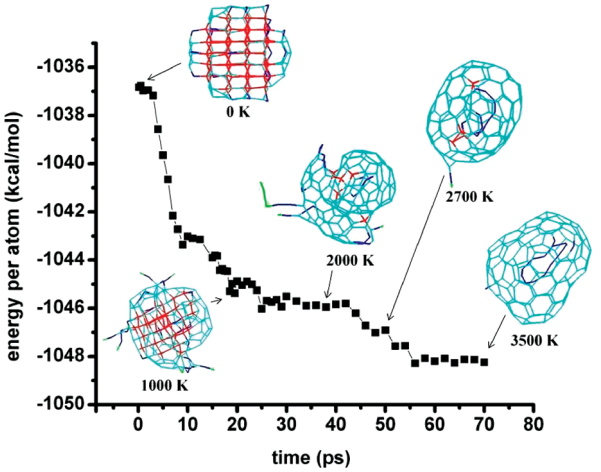

Figure 3. Structure transformation and energy profile of the spherical (311) nanodiamond cluster with 172 atoms as the initial structure. The sharp drop in energy is related to the first stage of transformation. The second stage refers to the plateau between 1000 and 2200 K. The interior atoms can come outside through the hole in the sp^2 envelope. The third stage is represented by the relative fast reduction in energy from 40 ps. This stage is clearly distinguished here. Red lines are sp^3 bonds, light blue lines are sp^2 bonds, and dark blue lines are sp bonds.

single-shell fullerene-like structures upon heating. The number of atoms, N_1 for the initial structure (N_2 for final structure), diameters, D_1 for the initial structure, equatorial diameters, D_2, and shape and orientation of initial nanodiamonds are listed in Table I. We collected the temperature in the Table I: T_1 when the inner core of nanodiamond starts to transform and T_2 when the closed-shell fullerene is formed. If closed-shell fullerenes contain an inner structures and "tails" at the temperature T_2, the heating will continue to remove the "tails" and inner structure for obtaining fullerenes with clean shape. Both T_1 and T_2 are higher as the size of nanodiamond cluster grows. In most of cases, the complete transformation of nanodiamond with more than 100 atoms requires temperature T_2 = 2500 K and above. Both T_1 and T_2 of spherical nanodiamonds are usually higher than those of cubic ones with the similar number of atoms. For example, the spherical cluster with 106 atoms' T_1 and T_2 are 700 and 2600 K, respectively, which is higher than that of cubic cluster with 101 atoms, that is, 500 and 1700 K. The orientation of nanodiamonds affects the transformation temperature as well, as shown in Table I. In terms of topological feature of these fullerenes, they consist of sp^2-hybridized carbon atoms and contain 4-, 5-, 6-, 7-, and even 8-membered rings. The isolated pentagon rule is violated for some fullerenes generated in our simulations, however these structures remain intact even at 3500 K during for 100 ps and the subsequent cooling. Two single-shell fullerenes contain only pentagons and hexagons. One has 44 atoms, obtained from cubic (111) nanodiamond with 63 atoms. The other has 60 atoms, obtained from spherical (001) nanodiamond with 66 atoms. Their topology satisfies the Euler's theorem,[83] that is, number of hexagons (h) and number of pentagons (p) of a fullerene C_n are related by the equation:

$$p + h = n/2 + 2 \quad (1)$$

If a fullerene contains pentagons, hexagons and heptagons only, then number of pentagons is $p = 12 + s$, where s is the number of heptagons. For fullerenes without heptagons, the number of pentagons is 12. Thus, the number of hexagons, h, equal to $n/2 - 10$, where n is a number of atoms. This rule works for our single-shell fullerenes with 44, 60, 68, 74, 88, and 126 atoms (see Table Ia). When the fullerenes have squares and octagons that are related to the presence of "tails", this theorem will not be obeyed.

3.2. Formation of Double-Shell (Onion-Like) Fullerenes. Experiments show that onion-like carbons could be synthesized by annealing diamond nanoparticles of diameter 2−10 nm[51−54] between 1100 and 1400 °C. In agreement with these experiments, our simulations show that, if the size of the initial spherical nanodiamond cluster is more than ∼200 atoms, the onion-like fullerene will be formed. The smallest diamond cluster that transforms into double shell onion fullerene is the 206 atoms spherical (111) nanodiamond cluster. The onion contains 164 atoms, 32 of them belong to the inner fullerene and 132 atoms belong to the outer fullerene. Both inner and outer fullerenes are stretched in the same direction. Almost all spherical nanodiamonds containing more than 200 atoms convert themselves into onions except one spherical (111) cluster with 220 atoms, which is transformed into single-shell fullerene. Interestingly, the shape dependence is manifested by the lower bound of smallest number of atoms in cubic nanodiamond cluster to form onion-like carbons. The cubic nanodiamonds as big as 229 and 293 atoms transform into single-shell fullerenes. It turns out to be 302 atoms, much larger than that of spherical cases. This shape dependence is due to the presence of a large amount of weakly bonded edge atoms in the initial cubic nanodiamonds. In the process of heating, these edge atoms are easily detached from the cluster, resulting in an insufficient number of atoms to form the onion structure.

The sizes of both the inner and outer shells in onions increase as the number of atoms of the initial cluster increases. Some onions have an intershell cross-links. Meanwhile, the intershell distance remains to be constant. The distance between two shells of our onion-like fullerenes varies from 2.6 to 4 Å. An average distance between two shells is 3.1 Å, which is smaller than

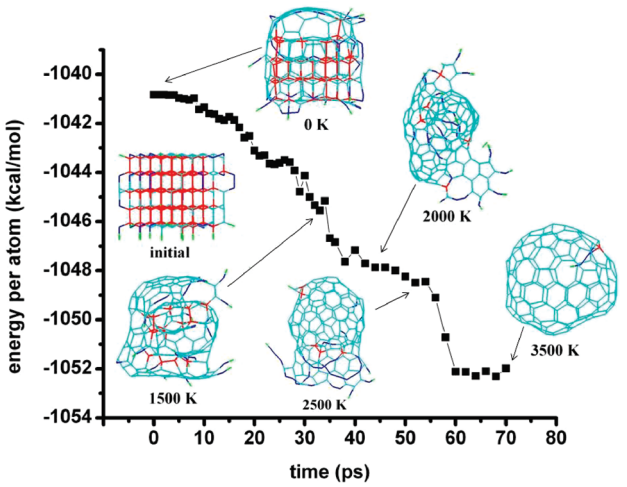

Figure 4. Structure transformation and energy profile of a cubic (111) nanodiamond cluster with 229 atoms as the initial structure. The upper and lower surfaces are transformed into graphitized ones during the optimization at 0 K, while the interior atoms remain the diamond order. During the first stage, the diamond core of the cluster has significant transformation to form the curved sp^2 envelop between upper and lower graphitic planes with a hole, and the energy reduces with a fast rate. Subsequently, the interior atoms keep transforming to the surface during the second stage, with a very slow rate in energy reduction. The third stage is represented by the relative fast reduction in energy from 50 ps. Red lines are sp^3 bonds, light blue lines are sp^2 bonds, and dark blue lines are sp bonds.

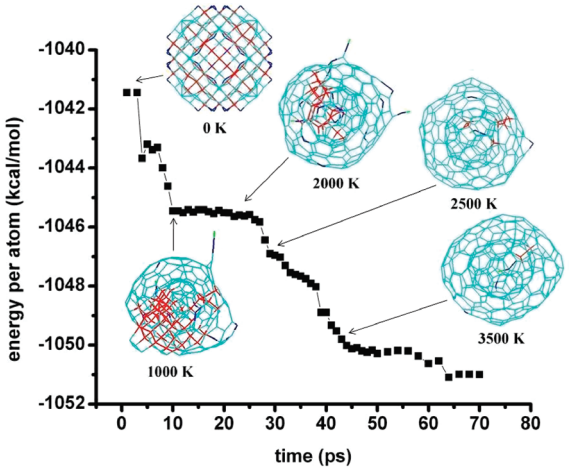

Figure 5. Structure transformation and energy profile of spherical (001) nanodiamond cluster with 256 atoms as initial structure. During the first stage, two sp^2 envelopes form: one is around the core, the other is on the outer surface. In the second stage, interior sp^3 atoms are converted to sp^2 through the holes. At the third stage, there is a prolonged fast drop of energy period after 25 ps, when the inner and outer fullerenes rearrange and change their topology by "direct adsorption" and the "push out" processes. Red lines are sp^3 bonds, light blue lines are sp^2 bonds, and dark blue lines are sp bonds.

graphite interlayer distance 3.35 Å, and on the lower bound of the experimental observations 3.1−3.5 Å.[19] The detailed information, including shape and orientation of initial nanodiamonds, N_1 (N_2), D_1, and two sets of equatorial diameters D_2 due to the presence of two shells in the onion structures, are listed in Table Ib. Topologically, the Euler's theorem is observed for the outer shell with 132 atoms of the onion with 164 atoms obtained from the spherical (111) cluster with the 206 atoms, and the inner shell with 62 atoms of the onion structure with 248 atoms, obtained from the spherical (001) cluster with 256 atoms.

3.3. Generic Three-Stage Transformation Dynamics. The heating induced transformation into fullerene starts when partial carbon atoms at the surface of the cluster undergo graphitization, followed by the sp^3 bond among interior diamond structure starts to break and join the sp^2 envelope on the surface. For the small nanodiamonds with up to 100 atoms, the process of formation of the envelope involves almost all atoms. Only a few disordered atoms remain inside the envelope. The stages of the transformation and the profile of energy per atom of a spherical nanodiamond cluster with 71 atoms as the initial structure are shown in Figure 2. The formation of the blue sp^2 envelope with a few inner atoms is clearly visible in Figure 2 at 800 K. The structures are stored for all the sampling points. The energy per atom is computed as one postsimulation task. For each structure, the cluster without detached carbon fragments is cooled down to the room temperature. Then the energy per atom is defined as the energy of the cluster at room temperature normalized by the number of atoms of this cluster. Here we highlight one very important observation: *three-stage transformation*. In Figure 2, one sharp drop of energy at the first stage of the transformation reflects the conversion of dangling bonds at the surface into sp^2 atoms, and the transformation of sp^3 into sp^2 bonds. The temperature of this stage ranges from 600 to 1000 K. The sp^2 envelope has a hole. Subsequently, the remaining interior atoms start to come out through the hole during the second stage. Some of them detach the cluster in the form of C_2 molecules or carbon chains, while part of them integrates into the envelope. The hole is very dynamic and stays open for an appreciable time. This stage is represented by the very slow decrease of energy between 10 and 20 ps, featured by the "flow-out process" of interior carbon atoms to the surface through the hole and the coexistence of a similar amount of sp^3 and sp^2 atoms, as shown in Figure 2. A few inner atoms remain inside the closed sp^2 envelope. At the third stage of transformation, the energy decreases fast. At further heating up to 3000 K these inner atoms come out, the system lost almost all remaining tails, and formation of fullerene is complete. This stage is not clearly distinguishable for small nanodiamonds with up to 100 atoms due to the limited number of remaining interior atoms. To present the more evident feature of the third stage, we choose one spherical nanodiamond cluster with 172 atoms whose evolution of the energy per atom and the stages of the transformation are presented in Figure 3. During the first stage, the formation of the sp^2 envelope with a hole occurs, accompanied by the fast reduction in terms of energy per atom, as shown in the structure at 1000 K in Figure 3. Then the decrease of the energy per atom slows down as in the second stage. A large amount of interior sp^3 atoms starts to convert themselves into sp^2 atoms and join the sp^2 envelope through the hole until the disappearance of the diamond core. For example, the structure shows a small fullerene inside a sp^2-bonded semisphere at 2000 K. Shortly after, the third stage of the transformation begins. The hole closes, and the outer semisphere integrates with the surface of the small fullerene to form one big closed-shape fullerene-like cage, as shown in the structure at 2700 K. Although many atoms detach from the surfaces during this process, the closed fullerene still has a number of atoms

inside. These atoms can be removed by further heating up to 3500 K through the "direct adsorption" and "push out" mechanisms.[39] In the "direct adsorption" process, interior atoms break bonds between the surface atoms, then form the new bonds with the surface atoms, and convert themselves into surface atoms. It contributes to the increase of the fullerene cage size. Besides, interior atoms push out surface atoms and stand on their places, which represents the "push out" process. During this stage, there is a fast drop of energy until no carbon atoms remain inside the closed fullerene,[84] as shown between 40 and 60 ps in Figure 3. Clearly, the third stage is more evident in this case due to the more atoms presented in the initial structure.

It is known from quantum simulations that the most effective way to minimize the surface free-energy of {111} surfaces of a diamond is by graphitization.[85] It is interesting to consider the transformation of a cubic nanodiamond cluster with {111} surfaces containing 229 atoms, as shown in Figure 4. Indeed, the upper and lower surfaces are transformed into graphitized ones during the optimization at 0 K, while the interior atoms remain the diamond order, as commonly observed in the reconstructed {111} surfaces. The diameter of the cluster slightly increases from 10.87 to 11.77 Å in the direction perpendicular to the {111} surfaces. Upon heating, the diamond core of the cluster has significant transformation to form a curved sp^2 envelop between upper and lower graphitic planes with a hole at 1500 K. During the first stage of transformation, the energy reduces with a relatively fast rate. Subsequently, the interior atoms keep transforming to the surface during the second stage. The upper and lower graphitic surfaces remain connected to the main cluster and form "wings" of the new-formed fullerene at 2000 K. The hole is located under the wings. Under further heating the wings integrate into the fullerene surface. Then the third stage starts when the hole close to form one big fullerene at 2500 K. The tails on the surface will detach from the cluster at higher temperature. The final structure has 178 atoms that form 25 five-, 43 six-, 13 seven-, and 5 eight-membered rings. We then analyze the transformation process of bigger nanodiamonds. If the initial nanodiamond carbon cluster has atoms over 200, the initial sp^2 envelope is so big that many interior atoms may not come out during the second and third stages of transformation. Thus, another small fullerene could be formed inside the sp^2 envelope, that is, a double-shell onion-like form. Furthermore, the "three-stage transformation" remains to be valid during the formation of the double-shell fullerene, as shown in Figure 5 for the formation of the onion-like carbon structure with 248 atoms. It is obtained from a spherical (001) nanodiamond with 256 atoms. At the first stage, the "flow out" mechanism is not very effective in this case. Although the hole on the outer surface fluctuates, interior atoms form an additional inner sp^2 envelop rather than come out through the hole. So, two sp^2 envelopes form by converting sp^3 atoms: one is around the core, the other is at the outer surface; as shown in the structure at 1000 K. During the second stage, remaining interior sp^3 atoms start to convert to sp^2. The plateau of the energy profile between 10 and 25 ps is related to this stage, where the inner and outer shells evolve separately. Then comes the third stage. The hole closes at 2500 K, and, more importantly, the "direct adsorption" and "push out" mechanisms start to work at 2500 K. These mechanisms are extremely effective for big nanodiamonds. The inner and outer fullerenes change their topology, and the number of cross-links between two shells decrease. The energy profile shows the prolonged decrease of energy related to the third stage of transformation from 25 to 65 ps. The final fullerene contains 62 atoms in the inner shell and 186 atoms in the outer shell at 3500 K. The energy profiles of the above two transformations clearly reveal the generic character of the *three-stage transformation.*

Considering that previous simulations of the transformation of nanodiamonds into fullerenes[37,39] have been carried out with instant heating up to the targeted temperature, 1400−2800[37] and 2500 K,[39] we perform addition simulations with instant heating to 2500 K in order to understand the influence of the heating rate on our results and, more importantly, on the proposed *three-stage transformation* mechanism. Interestingly, all nanodiamonds with 60 atoms and above transform into fullerenes at instant heating. However, the number of atoms in the simulated fullerene and its topology are different. For example, the cluster with 71 atoms with instant heating up to 2500 K transforms into one fullerene with 54 atoms containing 16 pentagons, 9 hexagons, and 4 heptagons (instead of the fullerene with 65 atoms containing 14 pentagons, 17 hexagons, 2 heptagons, and 1 octagon obtained by the gradual heating) during 18 ps. The cluster with 172 atoms transforms into a single-shell fullerene with 126 atoms with 17 pentagons, 41 hexagons, and 5 heptagons. The spherical nanodiamond cluster with 194 transforms into double-shell fullerene upon instant heating at 2500 K, while this cluster is converted to the single−shell fullerene in the case of the gradual heating. All spherical nanodiamonds, which has more than 194 atoms, transform into double-shell fullerenes at instant heating. However, the cubic cluster with 216 atoms forms the single-shell fullerene at both instant and gradual heating. Nonetheless, the "*three-stage transformation*" pathway holds for all the above instant heating simulations.

4. SUMMARY

We have performed the density-functional tight-binding simulations of nanodiamonds with various shapes and orientations with a diameter ranging from 5 to 14 Å under gradual heating and instant heating. The nanodiamonds with 60 and more atoms are converted into fullerene-like structures. The smallest fullerene-like structure obtained in this work contains 31 atoms. A number of the fullerenes consist of pentagons and hexagons only. A few others contains 7-membered rings. Many fullerene-like structures are highly distorted and contain 4-, 5-, 6-, 7-, and 8-membered rings. The transformation temperature depends on the size, shape, and orientation of the initial structure. The big nanodiamonds require higher temperature for the transformation. The temperature of transformation for cubic nanodiamonds is lower than for that of spherical ones with similar size. Spherical nanodiamonds with 200 atoms and above transform into double-shell onions. And the number of atoms in the initial cubic cluster required for forming onion is 302. An average intershell distance is 3.1 Å, which is at the lower bound of the experimental measurement. The final product is sensitive to heating rate. More interestingly, we have observed the "*three-stage transformation*" in all the simulations performed in this work. In the first stage, the sp^2 envelope forms by transforming sp^3 atoms with dangling bonds to sp^2 atoms accompanied by the canonical transformation from sp^3 to sp^2 bonds. This stage is featured by a sharp drop of energy. In the second stage, a part of the interior atoms can come outside through the hole in the sp^2 envelope. This "flow-out"

mechanism prevails in the transformation for small nanodiamonds with up to 100 atoms. The energy decreases slowly within the second stage of the transformation. At the third stage, the hole closes and the structure transforms into fullerene with a number of atoms remaining inside. These remaining atoms can come out as described by the "direct adsorption" and "push out" mechanisms, which are especially effective for big nanodiamonds. The energy decreases relatively fast in the third stage.

AUTHOR INFORMATION

Corresponding Author
*E- mail: hbsu@ntu.edu.sg.

ACKNOWLEDGMENT

We thank A. Horsfield for discussions on the PLATO package. We are grateful to P. M. Ajayan, H. J. Gao, X.-Y. Li, S. Yang, R. Kalish, and V. Sorkin for useful discussions. The research is supported by MoE Tier-2 (ARC 13/08) and A*STAR SERC grant (Grant No. M47070020).

REFERENCES

(1) Kroto, H. W.; Heath, J. R.; O'Brien, S. C.; Curl, R. F.; Smalley, R. E. *Nature* **1985**, *318*, 162–163.
(2) Krätschmer, W.; Lamb, L. D.; Fostiropoulos, K.; Huffman, D. R. *Nature* **1990**, *347*, 354–358.
(3) Iijima, S. *Nature* **1991**, *354*, 56–58.
(4) Novoselov, K. S.; Geim, A. K.; Morozov, S. V.; Jiang, D.; Zhang, Y.; Dubonos, S. V.; Grigorieva, I. V.; Firsov, A. A. *Science* **2004**, *306*, 666–669.
(5) Smith, B. W.; Monthioux, M.; Luzzi, D. E. *Nature* **1998**, *396*, 323–324.
(6) Nasibulin, A. G.; Pikhitsa, P. V.; Jiang, H.; Brown, D. P.; Krasheninnikov, A. V.; Anisimov, A. S.; Queipo, P.; Moisala, A.; Gonzalez, D.; Lientschnig, G.; Hassanien, A.; Shandakov, S. D.; Lolli, G.; Resasco, D. E.; Choi, M.; Tománek, D.; Kauppinen, E. I. *Nat. Nanotechnol.* **2007**, *3*, 156–161.
(7) Gerhardt, Ph.; Löffler, S.; Homann, K. H. *Chem. Phys. Lett.* **1987**, *137*, 306–310.
(8) Howard, J. B.; McKinnon, J. T.; Makarovsky, Y.; Lafleur, A. L.; Johnson, M. E. *Nature* **1991**, *352*, 139–141.
(9) Diederich, F.; Whetten, R. L. *Acc. Chem. Res.* **1992**, *25*, 119–126.
(10) Ugarte, D. *Nature* **1992**, *359*, 707–709.
(11) Daly, T. K.; Buseck, P. R.; Williams, P.; Lewis, C. F. *Science* **1993**, *259*, 1599–1601.
(12) Becker, L.; Bada, J. L.; Winans, R. E.; Hunt, J. E.; Bunch, T. E.; French, B. M. *Science* **1994**, *265*, 642–645.
(13) Heymann, D.; Chibante, L. P. F.; Brooks, R. R.; Wolbach, W. S.; Smalley, R. E. *Science* **1994**, *265*, 645–647.
(14) Miki-Yoshida, M.; Castillo, R.; Ramos, S.; Rendón, L.; Tehuacanero, S.; Zou, B. S.; José-Yacamán, M. *Carbon* **1994**, *32*, 231–246.
(15) Banhart, F.; Ajayan, P. M. *Nature* **1996**, *382*, 433–435.
(16) van Orden, A.; Saykally, R. J. *Chem. Rev.* **1998**, *98*, 2313–2358.
(17) Kietzmann, H.; Rochow, R.; Ganteför, G.; Eberhardt, W.; Vietze, K.; Seifert, G.; Fowler, P. W. *Phys. Rev. Lett.* **1998**, *81*, 5378–5381.
(18) Piskoti, C.; Yarger, J.; Zetti, A. *Nature* **1998**, *393*, 771–774.
(19) Ajayan, P. M. *Chem. Rev.* **1999**, *99*, 1787–1799.
(20) Li, Y. B.; Wei, B. Q.; Liang, J.; Yu, Q.; Wu, D. H. *Carbon* **1999**, *37*, 493–497.
(21) Prinzbach, H.; Weiler, A.; Landenberger, P.; Wahl, F.; Wörth, J.; Scott, L. T.; Gelmont, M.; Olevano, D.; Issendorff, B. V. *Nature* **2000**, *407*, 60–63.
(22) Becker, L.; Poreda, R. J.; Hunt, A. J.; Bunch, T. E.; Rampino, M. *Science* **2001**, *291*, 1530–1533.
(23) Chen, X. H.; Deng, F. M.; Wang, J. X.; Yang, H. S.; Wu, G. T.; Zhang, X. B; Peng, J. C.; Li, W. Z. *Chem. Phys. Lett.* **2001**, *336*, 201–204.
(24) Sano, N.; Wang, H.; Chhowalla, M.; Alexandrou, I.; Amaratunga, G. A. J. *Nature* **2001**, *414*, 506–507.
(25) Cataldo, F.; Keheyan, Y. *Fullerenes, Nanotubes, Carbon Nanostruct.* **2002**, *10*, 313–332.
(26) Sano, N.; Wang, H.; Alexandrou, I.; Chhowalla, M.; Teo, K. B. K.; Amaratunga, G. A. J.; Iimura, K. *J. Appl. Phys.* **2002**, *92*, 2783–2788.
(27) Thune, E.; Cabioc'h, Th.; Jaouen, M.; Bodart, F. *Phys. Rev. B* **2003**, *68*, 115434.
(28) Chhowalla, M.; Wang, H.; Sano, N.; Teo, K. B. K.; Lee, S. B.; Amaratunga, G. A. J. *Phys. Rev. Lett.* **2003**, *90*, 155504.
(29) Su, H. B.; Goddard, W. A., III; Zhao, Y. *Nanotechnology* **2007**, *17*, 5691–5695.
(30) Zhu, X.; Su, H. B. *Phys. Rev. B* **2009**, *79*, 165401.
(31) Robertson, D. H.; Brenner, D. W.; White, C. T. *J. Phys. Chem.* **1992**, *96*, 6133–6135.
(32) Chelikowsky, J. R. *Phys. Rev. B* **1992**, *45*, 12062–12070.
(33) Schweigert, V. A.; Alexandrov, A. L.; Morokov, Y. N.; Bedanov, V. M. *Chem. Phys. Lett.* **1995**, *235*, 221–229.
(34) Strout, D. L.; Scuseria, G. E. *J. Phys. Chem.* **1996**, *100*, 6492–6498.
(35) László, I. *Europhys. Lett.* **1998**, *44*, 741–746.
(36) Yamaguchi, Y.; Maruyama, S. *Chem. Phys. Lett.* **1998**, *286*, 336–342.
(37) Fugaciu, F.; Hermann, H.; Seifert, G. *Phys. Rev. B* **1999**, *60*, 10711–10714.
(38) Mishra, R. K.; Lin, Y. -T.; Lee, S. -L. *J. Chem. Phys.* **2000**, *112*, 6355–6364.
(39) Lee, G.-D.; Wang, C. Z.; Yu, J.; Yoon, E.; Ho, K. M. *Phys. Rev. Lett.* **2003**, *91*, 265701.
(40) Zheng, G; Irle, S.; Morokuma, K. *J. Chem. Phys.* **2005**, *122*, 014708.
(41) Khan, S. D.; Ahmad, S. *Nanotechnology* **2006**, *17*, 4654–4658.
(42) Irle, S.; Zheng, G.; Wang, Z.; Morokuma, K. *J. Phys. Chem. B* **2006**, *110*, 14531–14545.
(43) Bródka, A.; Zerda, T. W.; Burian, A. *Diam. Relat. Mater.* **2006**, *15*, 1818–1821.
(44) Su, H. B.; Nielsen, R. J.; van Duin, A.; Goddard, W. A., III *Phys. Rev. B* **2007**, *75*, 134107.
(45) Bogana, M. P.; Colombo, L. *Appl. Phys. A: Mater. Sci. Process.* **2007**, *86*, 275–281.
(46) Lau, D. W. M.; McCulloch, D. G.; Marks, N. A.; Masden, N. R.; Rode, A. V. *Phys. Rev. B* **2007**, *75*, 233408.
(47) Bródka, A.; Hawełek, Ł.; Burian, A.; Tomita, S.; Honkimäki, V. *J. Mol. Struct.* **2008**, *887*, 34–40.
(48) Leyssale, J. −M.; Vignoles, G. L. *Chem. Phys. Lett.* **2008**, *454*, 299–304.
(49) Powles, R. C.; Marks, N. A.; Lau, D. W. M. *Phys. Rev. B* **2009**, *79*, 075430.
(50) Chevrot, G.; Bourasseau, E.; Pineau, N.; Maillet, J. −B. *Carbon* **2009**, *47*, 3392–3402.
(51) Kuznetsov, V. L.; Chuvilin, A. L.; Butenko, Yu. V.; Mal'kov, I. Yu.; Titov, V. M. *Chem. Phys. Lett.* **1994**, *222*, 343–348.
(52) Tomita, S.; Sakurai, T.; Ohta, H.; Fujii, M.; Hayashi, S. *J. Chem. Phys.* **2001**, *114*, 7477–7482.
(53) Gruen, D. M.; Shenderova, O. A.; Vul', A. Ya. *Synthesis, Properties and Applications of Ultrananocrystalline Diamond*; NATO Science Series; Springer: New York, 2005.
(54) Qiao, Z.; Li, J.; Zhao, N.; Shi, C.; Nash, P. *Scr. Mater.* **2006**, *54*, 225–229.
(55) Butenko, Yu. V.; Kuznetsov, V. L.; Paukshtis, E. A.; Stadnichenko, A. I.; Mazov, I. N.; Moseenkov, S. I.; Boronin, A. I.; Kosheev, S. V. *Fullerenes, Nanotubes, Carbon Nanostruct.* **2006**, *14*, 557–554.
(56) Baidakova, M.; Vul', A. *J. Phys. D: Appl. Phys.* **2007**, *40*, 6300–6311.

(57) Winter, N. W.; Ree, F. H. *J. Comput.-Aided Mater. Des.* **1998**, *5*, 279–294.
(58) Ree, F. H.; Winter, N. W.; Glosli, J. N.; Viecelli, J. A. *Phys. B (Amsterdam, Neth.)* **1999**, *265*, 223–229.
(59) Hermann, H.; Fugaciu, F.; Seifert, G. *Appl. Phys. Lett.* **2001**, *79*, 63–65.
(60) Barnard, A. S.; Russo, S. P.; Snook, I. K. *J. Chem. Phys.* **2003**, *118*, 5094–5097.
(61) Barnard, A. S.; Russo, S. P.; Snook, I. K. *Diamond Relat. Mater.* **2003**, *12*, 1867–1872.
(62) Raty, J. -Y.; Galli, G. *Nat. Mater.* **2003**, *2*, 792–795.
(63) Raty, J. −Y.; Galli, G.; Bostedt, C.; van Buuren, T. W.; Terminello, L. J. *Phys. Rev. Lett.* **2003**, *90*, 037401.
(64) Frauenheim, Th.; Weich, F.; Köhler, Th.; Uhlmann, S. *Phys. Rev. B* **1995**, *52*, 11492–11501.
(65) Widany, J.; Weich, F.; Köhler, Th.; Porezag, D; Frauenheim, Th. *Diam. Relat. Mater.* **1996**, *5*, 1031–1041.
(66) Horsfield, A. P. *Phys. Rev. B* **1997**, *56*, 6594–6602.
(67) Horsfield, A. P.; Bratkowsky, A. M. *J. Phys.: Condens. Matter* **2000**, *12*, R1–R24.
(68) Kenny, S. D.; Horsfield, A. P.; Fujitani, H. *Phys. Rev. B* **2000**, *62*, 4899–4905.
(69) Frauenheim, Th.; Jungnickel, G.; Köhler, Th.; Stephan, U. *J. Non-Cryst. Solids* **1995**, *182*, 186–197.
(70) Kohary, K.; Kugler, S.; Hajnal, Z.; Köhler, Th.; Frauenheim, Th.; Kátai, S.; Deák, P. *Diamond Relat. Mater.* **2002**, *11*, 513–518.
(71) Yao, Y.; Liao, M. Y.; Köhler, Th.; Frauenheim, Th.; Zhang, R. Q.; Wang, Z. G.; Lifshitz, Y.; Lee, S. T. *Phys. Rev. B* **2005**, *72*, 035402.
(72) Jungnickel, G.; Latham, C. D.; Heggie, M. I.; Frauenheim, Th. *Diamond Relat. Mater.* **1995**, *5*, 102–107.
(73) Frauenheim, Th.; Köhler, Th.; Sternberg, M.; Porezag, D.; Pederson, M. R. *Thin Solid Films* **1996**, *272*, 314–330.
(74) Astala, R.; Kaukonen, M.; Nieminen, R. M.; Jungnickel, G.; Frauenheim, Th. *Phys. Rev. B* **2001**, *63*, 081402.
(75) Mehrez, H.; Svizhenko, A.; Anantram, M. P.; Elstner, M.; Frauenheim, Th. *Phys. Rev. B* **2005**, *71*, 155421.
(76) Lin, C. S.; Zhang, R. Q.; Niehaus, T. A.; Frauenheim, Th. *J. Phys. Chem. C* **2007**, *111*, 4069–4073.
(77) Malola, S.; Häkkinen, H.; Koskinen, P. *Phys. Rev. B* **2008**, *77*, 155412.
(78) Becke, A. D. *Phys. Rev. A* **1988**, *38*, 3098–3100.
(79) Lee, C.; Yang, W.; Parr, R. G. *Phys. Rev. B* **1988**, *37*, 785–789.
(80) Becke, A. D. *J. Chem. Phys.* **1993**, *98*, 5648–5652.
(81) Humphrey, W.; Dalke, A.; Schulten, K. *J. Mol. Graphics* **1996**, *14*, 33–38.
(82) Adler, J.; Hashibon, A.; Schreiber, N.; Sorkin, A.; Sorkin, S.; Wagner, G. *Comput. Phys. Commun.* **2002**, *147*, 665–669.
(83) Fowler, P. W.; Manolopoulos, D. E. *An Atlas of Fullerenes*; Dover Publication Inc.: Mineola, NY, 2006.
(84) Under some circumstances, part of the interior atoms still remain inside the fullerene even after 70 ps at the temperature of 3500 K. In these cases the final fullerenes contain carbon fragments, that is, molecules C_2, carbon chains of 3−7 atoms, and even small rings. For example, the fullerene with 124 atoms, obtained from the nanodiamond cluster with 172 atoms, contains 11-fold ring inside as shown by the dark blue ring inside the fullerene at 3500 K in Figure 4.
(85) De Vita, A.; Galli, G.; Canning, A.; Car, R. *Nature* **1996**, *379*, 523–526.